

Automatic Generation of Accurate and Cost-efficient Auxiliary Basis Sets

Susi Lehtola^{*,†,‡}

[†]*Molecular Sciences Software Institute, Blacksburg, Virginia 24061, United States*

[‡]*Department of Chemistry, University of Helsinki, P.O. Box 55, FI-00014 University of Helsinki, Finland*

E-mail: susi.lehtola@alumni.helsinki.fi

Abstract

We have recently discussed an algorithm to automatically generate auxiliary basis sets (ABSs) of the standard form for density fitting (DF) or resolution-of-the-identity (RI) calculations in a given atomic orbital basis set (OBS) of any form [J. Chem. Theory Comput. 2021, 17, 6886]. In this work, we study two ways to reduce the cost of such automatically generated ABSs without sacrificing their accuracy. We compactify the ABS with a singular value decomposition using a method proposed by Kállay [J. Chem. Phys. 2014, 141, 244113], which offers a rigorous way to throw away unimportant eigenvectors in the auxiliary basis. We also drop the high-angular momentum functions that are unnecessary for global fitting methods from the ABS. Studying the effect of these two types of truncations on Hartree–Fock (HF) and second-order Møller–Plesset perturbation theory (MP2) calculations on a chemically diverse set of first- and second-row molecules within the RI/DF approach, we show that accurate total and atomization energies can be achieved by a combination of the two approaches with significant reductions in the size of the ABS. While the original approach yields ABSs whose number of functions $N_{\text{bf}}^{\text{ABS}}$ scales with the number of functions in the OBS $N_{\text{OBS}}^{\text{bf}}$ as $N_{\text{ABS}}^{\text{bf}} = \gamma N_{\text{OBS}}^{\text{bf}}$ with the prefactor $\gamma \approx \mathcal{O}(10)$, the reduction schemes of this work afford results of essentially the same quality as the original unpruned ABS with $\gamma \approx 5$ –6, while

an accuracy that may suffice for routine applications is achievable with a further reduced ABS with $\gamma \approx 3$ –4.

1 Introduction

The density fitting^{1–5} (DF) also known as the resolution of the identity⁶ (RI) technique has become one of the mainstays of quantum chemistry. The DF/RI approach is widely available in many program packages as an optional technique to accelerate self-consistent field (SCF) as well as post-Hartree–Fock calculations. It is also used by default in some packages, such as Psi4⁷, while other packages like BAGEL⁸ and Demon2K⁹ go even further by relying solely on the use of DF/RI for all calculations, foregoing traditional routines based on the conventional electron repulsion integrals (ERIs) that are typically written in the Mulliken notation as

$$(\mu\nu|\sigma\rho) = \int \frac{\chi_{\mu}(\mathbf{r})\chi_{\nu}(\mathbf{r})\chi_{\sigma}(\mathbf{r}')\chi_{\rho}(\mathbf{r}')}{|\mathbf{r} - \mathbf{r}'|} d^3r d^3r' \quad (1.1)$$

where μ , ν , σ , and ρ are indices of atomic-orbital basis functions χ_{μ} that together span the orbital basis set (OBS).

In the DF/RI approach, the two-electron integrals of the OBS are approximated with the help of an auxiliary basis set (ABS) as⁶

$$(\mu\nu|\sigma\rho) \approx \sum_{AB} (\mu\nu|A)(A|B)^{-1}(B|\sigma\rho), \quad (1.2)$$

where A and B are functions in the ABS and $(A|B)^{-1}$ denotes the A, B element of the inverse of the two-index Coulomb overlap matrix $(A|B)$. Traditionally, ABSs are manually optimized for ground-state energy calculations for each OBS for each level of theory, but some automatic algorithms for generating an ABS from the given OBS have also been suggested;^{10–15} see ref. 16 for a recent review.

While some of these automated schemes inherently assume the use of Gaussian basis sets,^{11,12,14} we recently suggested an automated algorithm which can be used with any type of atomic-orbital basis set. In short, the central idea of this scheme is to generate the ABS by choosing it such that it spans all one-center products $\chi_\mu\chi_\nu$ in the OBS to a given degree of precision.

Because the one-center OBS products $\chi_\mu\chi_\nu$ can couple to angular momentum $|l_\mu - l_\nu| \leq L \leq l_\mu + l_\nu$, where l_μ and l_ν are the angular momenta of the functions χ_μ and χ_ν , respectively, the algorithm of ref. 15 works by assembling a list of normalized product radial functions

$$R_I^L(r) = N_I \chi_{\mu_I}(r) \chi_{\nu_I}(r) \quad (1.3)$$

for all possible angular momenta L in the auxiliary basis set, which serve as auxiliary basis function candidates. N_I is the normalization coefficient in eq. (1.3). The product radial functions can be prescreened by a pivoted Cholesky decomposition of the ERI tensor;¹⁷ this yields a more compact auxiliary basis set at no loss in accuracy.¹⁵

Next, the algorithm chooses the set of auxiliary radial functions for each angular momentum L , $R_I^L(r)$, by a pivoted Cholesky decomposition of the one-center Coulomb overlap matrix $(R_I^L|R_J^L)$, motivated by earlier work of Aquilante et al.¹² The decomposition is carried out to the given threshold τ ; a similar technique also works to cure overcompleteness in OBSs.^{18,19} Choosing the basis functions by a pivoted Cholesky decomposition of the (Coulomb) overlap matrix is analogous to using an optimal Gram–Schmidt orthogonalization.¹⁶

The algorithm of ref. 15 is applicable to any atomic-orbital basis sets: the necessary equa-

tions to compute the one-center Coulomb overlap matrix for Gaussian-type orbitals (GTOs) as well as Slater-type orbitals (STOs) were given in ref. 15, while the necessary integrals for numerical atomic orbitals²⁰ can easily be computed by quadrature.²¹

Because the cost of DF/RI methods scales linearly with the size of the ABS, automatically generated ABSs can be extremely useful for practical applications, as even if automatically generated ABSs tend to be large compared to their possible manually optimized counterparts, they already allow access to the correct asymptotic scaling in the size of the OBS shared by all DF/RI methods, enabling significant speedups in calculations compared to the use of the exact TEIs.

For this reason, our previous study¹⁵ focused on showing that negligible errors in Hartree–Fock (HF) and second-order Møller–Plesset perturbation theory (MP2) total energies could be achieved with the technique proposed therein in GTO basis set calculations, where the exact values without the DF/RI approximation are straightforward to compute.¹⁵ In this work, we will focus on improving the cost-efficiency of the automatically generated ABS. We will accomplish this along two routes.

First, we will consider contracting the ABS employing a singular value decomposition (SVD), which was originally suggested by Kállay²² to reduce the cost of RI/DF methods in general. The contraction of the ABS serves to restore the energetic connection of the auto-generated basis to the two-electron integrals, which was severed in the algorithm of ref. 15 that was laid out above. In addition to allowing the generation of contracted Gaussian auxiliary basis sets for contracted Gaussian orbital basis sets, the contraction procedure is also seen to be beneficial in combination with uncontracted Gaussian basis sets, and likely other types of atomic basis sets, as well.

Second, we will also consider two schemes to discard high-angular momentum (HAM) functions from the ABS: in addition to the scheme used by previous automated schemes (refs. 11 and 14), we will also discuss a first-principles scheme, which has been previously discussed in

the context of optimized ABSs.²³ As we will demonstrate in this work, the HAM functions can be safely discarded in global fitting methods, as they have negligible effect on total and relative energies.

The layout of this work is the following. Next, in section 2, we will discuss the theory behind the present approach: the contraction of the ABS is discussed in section 2.1, while the pruning of HAM functions is discussed in section 2.2. The computational details of the benchmarking based on HF and MP2 calculations are given in section 3. The results of the study are discussed in section 4, and the study concludes in a brief summary and discussion in section 5. Atomic units are used throughout, unless specified otherwise.

2 Theory

2.1 Contracted sets

For clarity, we will reuse the notation used by Kállay²², who writes eq. (1.2) in the form

$$\mathcal{I} \approx \mathbf{I} \mathbf{V}^{-1} \mathbf{I}^T \quad (2.1)$$

where $\mathcal{I}_{\mu\nu,\rho\sigma} = (\mu\nu|\rho\sigma)$ is the ERI tensor, $I_{\mu\nu,A} = (\mu\nu|A)$ are the three-index integrals and $V_{A,B} = (A|B)$ are the two-index Coulomb overlap integrals. Equation (2.1) can be expressed in a more compact form in the orthogonalized ABS: defining orthogonalized three-index integrals,

$$\mathbf{J} = \mathbf{I} \mathbf{V}^{-1/2} \quad (2.2)$$

eq. (2.1) is given simply by

$$\mathcal{I} \approx \mathbf{J} \mathbf{J}^T. \quad (2.3)$$

Kállay²² pointed out that the size of the auxiliary basis can be reduced by a SVD of \mathbf{J} by throwing out vectors with suitably small singular values, and that the singular values can be computed as the eigenvalues of the symmetric matrix

$$\mathbf{W} = \mathbf{J}^T \mathbf{J} \quad (2.4)$$

which has the dimension $N_{\text{aux}} \times N_{\text{aux}}$ where N_{aux} is the number of auxiliary basis functions. Be-

cause the number of auxiliary functions typically scales as the number of orbital basis functions, eq. (2.4) can be diagonalized even in large calculations.

However, in this work we consider using the above method to contract the auxiliary basis, which merely requires forming \mathbf{W} in an atomic calculation for a single element; the contracted auxiliary basis set is formed by the ensemble of such contracted elemental basis sets.

Because the \mathbf{W} matrix defined by eq. (2.4) is obtained by summing over all OBS products on the element, \mathbf{W} turns out to have a special angular structure. The only significant values are found when the angular momenta of the bra and ket basis functions coincide, $l' = l$ and $m' = m$, the other elements of \mathbf{W} being numerically zero. As one could expect, all spatial directions are therefore averaged in \mathbf{W} .

Because of this special structure, it suffices to compute, e.g., the $m' = 0 = m$ subblock of the $l = l'$ angular submatrix of \mathbf{W} , which we denote as $\mathbf{W}^{(l)}$, which contains information on the importance of the radial auxiliary functions of angular momentum l .

The eigendecomposition of $\mathbf{W}^{(l)}$ then yields

$$\mathbf{W}^{(l)} = \mathbf{U}^{(l)} \mathbf{\Lambda}^{(l)} \left(\mathbf{U}^{(l)} \right)^T, \quad (2.5)$$

where $\mathbf{\Lambda}^{(l)}$ is a diagonal matrix of eigenvalues and $\mathbf{U}^{(l)}$ is the corresponding matrix of eigenvectors. Now, we can choose the eigenvectors $\mathbf{U}_i^{(l)}$ with $\Lambda_i^{(l)} \geq \epsilon$ as our reduced ABS. This ABS has a guarantee of accuracy for the studied system, as the three-index integrals are reproduced to the precision specified by ϵ .

The contraction algorithm is thus the following:

1. Define truncation threshold ϵ and read in OBS and ABS.
2. Loop over atoms, and the atomic angular momentum l in ABS
 - (a) Form the angular subblock $\mathbf{W}_{lm,l'm'}$ for $l = l'$ and $m = 0 = m'$ from eq. (2.4), denoted as \mathbf{W}_l .
 - (b) Compute the eigenvectors \mathbf{w}_l and eigenvalues \mathbf{v}_l of \mathbf{W}_l .

- (c) Include eigenvectors \mathbf{w}_l with eigenvalue $v_l \geq \epsilon$ in the auxiliary basis.
- (d) Convert the eigenvectors into the non-orthonormal basis by $\mathbf{C}_l = \mathbf{V}_l^{-1/2} \mathbf{w}_l$.

To extract the contraction coefficients of a contracted GTO basis, a further step is necessary. As Gaussian basis functions are by convention tabulated in terms of primitives normalized in the overlap metric, while the coefficients of the eigenvectors \mathbf{w}_l correspond to Coulomb normalized primitives, one has to convert the contraction coefficients. This is achieved by scaling the coefficient of the μ :th Gaussian primitive in the i :th auxiliary function $C_{\mu i}$ by the square root of the corresponding Gaussian exponent, $C_{\mu i} \rightarrow C_{\mu i} \sqrt{\alpha_\mu}$, see the Appendix for derivation.

2.2 Pruned Angular Momentum

By default, automatically generated basis sets arising from a large orbital basis set may contain functions of extremely HAM, as an orbital basis with maximum angular momentum $l_{\text{OBS}}^{\text{max}}$ will give rise to orbital products with maximum angular momentum $2l_{\text{OBS}}^{\text{max}}$. For instance, a polarized quintuple- ζ basis for the oxygen atom ($l_{\text{OBS}}^{\text{max}} = 5$) will lead to an auxiliary basis set with up to $l = 10$ functions.

Such functions are problematic with in Gaussian-basis programs, as most programs do not implement integrals to such HAM. Moreover, since Gaussian integrals are typically computed in the cartesian Gaussian basis, computing integrals with HAM functions is extremely costly: the number of cartesian functions of angular momentum l is $(l+1)(l+2)/2$ compared to $2l+1$ for spherical functions. Furthermore, the HAM functions' contributions to total ground state energies tend to be negligible. This motivates removing them from the ABS altogether by a pruning procedure.

The question of what HAM functions can be removed is best approached by asking the opposite question: what are the functions which should never be pruned from the ABS? Even in highly excited states, most of the total energy

arises from orbitals that are occupied in the atomic ground state. The correct description of occupied orbitals being of key importance, the pruned auxiliary basis set should therefore reproduce (i) the highly energetic interactions of the atom's occupied orbitals with each other, as well as (ii) the interactions of the atom's occupied orbitals with its unoccupied orbitals, which are important for polarization and correlation effects in polyatomic systems.

Criterion (i) is automatically satisfied, if all products of occupied orbitals are correctly reproduced by the auxiliary basis set. Therefore, we demand that the angular momentum kept in the auxiliary basis $l_{\text{keep}}^{\text{max}}$ is at least double the maximum angular momentum of occupied shells in the ground state of the atom $l_{\text{occ}}^{\text{max}}$, $l_{\text{keep}}^{\text{max}} \geq 2l_{\text{occ}}^{\text{max}}$.

Yang et al.¹¹ define $l_{\text{occ}}^{\text{max}}$ as having the values 0, 1, 2, and 3 for $Z \leq 2$, $3 \leq Z \leq 18$, $19 \leq Z \leq 54$, and $Z \geq 55$, respectively, while Stoychev et al.¹⁴ use the ranges $Z \leq 2$, $3 \leq Z \leq 20$, $21 \leq Z \leq 56$, and $Z \geq 57$, respectively. That is, while both Yang et al.¹¹ and Stoychev et al.¹⁴ include p functions for the pre- d Li and Be atoms, the former likewise add d and f functions for the pre- d and pre- f alkali and alkaline atoms, respectively, while the latter do not. We will follow Yang et al.¹¹ and include d and f functions for K and Ca, and Cs and Ba, respectively.

Criterion (ii) for the minimal accuracy of the auxiliary basis set satisfied, if the auxiliary basis is able to accurately describe products of an occupied atomic orbital with any other orbital. Denoting the maximum angular momentum of the orbital basis by $l_{\text{OBS}}^{\text{max}}$, the second condition is seen to be satisfied by $l_{\text{keep}}^{\text{max}} \geq l_{\text{occ}}^{\text{max}} + l_{\text{OBS}}^{\text{max}}$.

The two criteria must be satisfied simultaneously, which is why we choose

$$l_{\text{keep}}^{\text{max}} = \max(2l_{\text{occ}}^{\text{max}}, l_{\text{occ}}^{\text{max}} + l_{\text{OBS}}^{\text{max}} + l_{\text{inc}}), \quad (2.6)$$

where l_{inc} is an adjustable parameter. As far as we are aware, this criterion has not been studied in the literature in the context of automatic generation of auxiliary basis sets, although a similar discussion can be found in the work of Weigend²³ discussing the optimization

of auxiliary basis sets. (The implementation of the atomic Cholesky procedures of Aquilante et al.¹⁰ and Aquilante et al.¹² in the OpenMolcas program²⁴ does include optional pruning of the angular momentum to a maximum defined by the auxiliary basis sets of Weigend²³; however, this procedure does not appear to be fully documented.)

In contrast, the work of Yang et al.¹¹ on Coulomb fitting limited the maximum angular momentum by

$$l_{\text{Yang}}^{\text{max}} = \max(2l_{\text{occ}}^{\text{max}}, l_{\text{OBS}}^{\text{max}} + l_{\text{inc}}) \quad (2.7)$$

and employed $l_{\text{inc}} = 1$ for all elements, while Stoychev et al.¹⁴ similarly employed eq. (2.7) with $l_{\text{inc}} = 1$ for elements up to Ar and 2 for other elements.

Our truncation scheme (eq. (2.6)) is seen to have important differences from that used by Yang et al.¹¹ and Stoychev et al.¹⁴ (eq. (2.7)): eq. (2.6) includes the atomic angular momentum and naturally employs a larger angular momentum cutoff for heavier elements. We will compare the two schemes for truncating the angular momentum defined by eqs. (2.6) and (2.7) in section 4.1, examining various values for l_{inc} and comparing the results to ones obtained with the full, unpruned autogenerated auxiliary basis.

3 Computational Details

The computational details of this work are similar to those of ref. 15. As in the previous work, we will examine the accuracy of the scheme on the triple- ζ to quintuple- ζ nZaPa-NR basis sets of Ranasinghe and Petersson²⁵, for which optimized auxiliary basis sets have not been reported in the literature. These OBSs were obtained from the Basis Set Exchange,²⁶ in whose Python backend we previously implemented the AutoAux procedure of Stoychev et al.¹⁴ which will again be used as a state-of-the-art point of reference.¹⁵

The full primitive ABSs were generated with ERKALE^{27,28} following the procedure of ref. 15, employing the threshold $\tau = 10^{-7}$ for the pivoted Cholesky decomposition. The contrac-

tion and reduction schemes presented above in section 2 were implemented in ERKALE^{27,28} in this work, and they are freely and openly available on GitHub. The employed values for the contraction and reduction parameters, ϵ and l_{inc} , respectively, are discussed in section 4.

Our previous work¹⁵ studied HF and MP2 total energies in the non-multireference part of the W4-17 test set²⁹ and showed that their RI/DF errors can be made negligible by the use of suitably large primitive auxiliary basis sets. As the auxiliary basis sets generated by the previously suggested automated procedure are already known to be transferable,¹⁵ and the contraction and reduction schemes of section 2 are based on mathematical principles, we will study here the chemically diverse subset of first- and second-row molecules from the database of Weigend and Ahlrichs³⁰, which has been previously used to assess DF/RI auxiliary basis sets for Hartree-Fock.²³ We limit the calculations to molecules containing at most nine atoms, which suffices to demonstrate the accuracy of the reduced basis sets.

As the employed spin states for the molecules are not documented in refs. 23 and 30, we decided to run HF and MP2 calculations for the Al (doublet), Be, B (doublet), Cl (doublet), C (triplet), F (doublet), H (doublet), Li (doublet), Mg, Na (doublet), N (quartet), O (triplet), P (quartet), Si (triplet), and S (triplet) atoms, and the AlN (triplet), BeS (triplet), Cl₂, ClF, CO, F₂, H₂, HCl, HF, Li₂, LiCl, LiF, LiH, MgF (doublet), N₂, NaCl, NaF, NaH, P₂, S₂ (triplet), BeH₂, CO₂, CS₂, H₂O, HCN, HCP, HNC, HNO, HSH, Li₂O, LiSLi, MgCl₂, MgF₂, MgH₂, Na₂O (triplet), Na₂S, OF₂, SF₂, SiO₂, SiS₂, AlCl₃, AlF₃, AlH₃, Be₄, BF₃, BH₃, C₂H₂, CH₂O, ClF₃, H₂O₂, HNO₂, HSSH, Mg₄, N₂H₂, N₄, Na₃N (triplet), Na₃P (triplet), NF₃, NH₃, PF₃, PH₃, PLi₃, Al₂O₃, Al₂S₃, CF₄, CH₂O₂, CH₃N, CH₄, HNO₃, S₅, SF₄, SiCl₄, SiF₄, SiH₄, Be₂F₄, Be₂H₄, BH₃CO, C₂H₃N, C₂H₄, CH₃OH, H₂CO₃, LiBH₄, N₂H₄, NH₄F, PF₅, H₂SO₄, SF₆, B₂H₆, B₄H₄, BH₃NH₃, C₂H₆, C₄H₄, H₃PO₄, Li₄Cl₄, Li₄H₄, Li₈, BeC₂H₆, and BeF₂O₂H₄ molecules. Altogether, the assessment therefore includes 113 systems, composed of 15 atoms and 98 molecules.

Conventional HF and MP2 calculations were performed for these molecules with the Gaussian’16 program;³¹ modifications of the basis set were disabled with `IOp(3/60=-1)`. The RI/DF calculations were carried out with Psi4.⁷ The basis set linear dependence threshold was set to 10^{-7} in both programs.

As our test systems only include first- and second-row molecules, the same value of l_{inc} is used for all elements in eq. (2.7) in our test calculations; note that Yang et al.¹¹ and Stoychev et al.¹⁴ similarly use $l_{\text{inc}} = 1$ for all elements up to argon.

4 Results

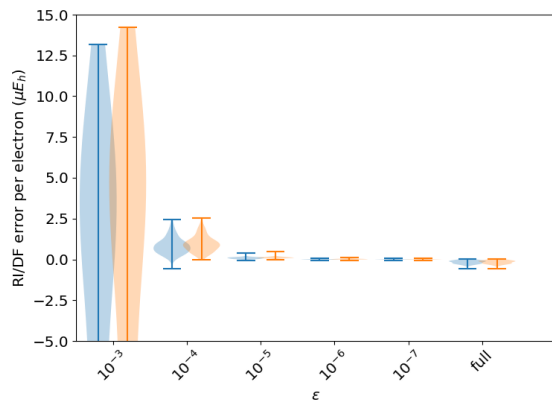
4.1 Detailed Analysis in the 3ZaPa-NR Basis Set

We begin by analyzing how RI/DF errors in HF and MP2 total and atomization energies are affected by contracting the auxiliary basis set according to the procedure of section 2.1, when the 3ZaPa-NR OBS is used. Because the DF/RI error is an extensive quantity, we will examine errors in total energies *per electron*, and errors in atomization energies *per atom*.

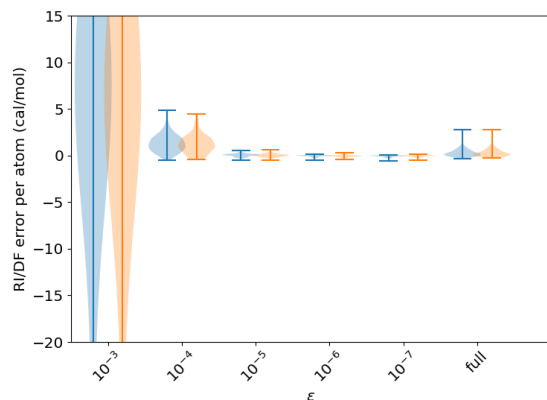
The RI/DF errors of the studied test set are shown as a function of the contraction threshold in fig. 4.1 for HF and MP2 total and atomization energies. The RI/DF errors converges rapidly when the contraction threshold ϵ is decreased. We observe that already the contraction threshold $\epsilon = 10^{-4}$ affords RI/DF errors in the order of a few μE_h per electron in total energies, and a few cal/mol per atom in atomization energies, which are negligible compared to the truncation error of the OBS and the inherent errors in the employed levels of theory.

It is also important to note here that the HF and MP2 errors behave very similarly as a function of ϵ . This result is fully expected for the contraction based on a SVD of the three-index integrals: because all integral classes are treated on the same footing, the error is not expected to depend on the examined level of theory.

Interestingly, the RI/DF errors afforded by



(a) Total energies



(b) Atomization energies

Figure 4.1: The effect of contraction on the RI/DF errors in the HF and MP2 total and atomization energies of the studied molecules in the 3ZaPa-NR basis set. The last entry in the violin plot shows the error distribution for the full, parent auxiliary basis set.

small values of ϵ are smaller than those obtained with the full parent auxiliary basis set. This difference can likely be attributed to the better conditioning of the contracted auxiliary basis set: unlike the parent ABS, the functions of the contracted ABS are orthonormal on each atom, leading to improved numerical stability in the RI/DF method when the contracted ABS is used in polyatomic calculations; this in turn reduces numerical errors.

We move on to studying the effect of pruning HAM auxiliary functions according to eqs. (2.6) and (2.7). The results of these procedures on HF and MP2 total and atomization energies are shown in fig. 4.2.

The value $l_{\text{inc}} = 0$ yields good results with eq. (2.6): although the MP2 total energy exhibits a small maximum absolute error of some $13 \mu E_h$ per electron (which arises for H_2), the HF total energies appear to be small and close to those from the full original ABS.

In contrast, the value $l_{\text{inc}} = 0$ yields unacceptably large errors for eq. (2.7): for instance, the MP2 total energy of the nitrogen atom is off by $-223 \mu E_h$ per electron and the MP2 atomization energy of P_2 is off by -893 cal/mol per atom.

Because eq. (2.7) clearly exhibits the wrong physical behavior, for the rest of this work we will consider only eq. (2.6) for pruning the HAM functions. With this scheme, $l_{\text{inc}} = 0$ already yields good accuracy, and the values with $l_{\text{inc}} = 1$ are almost converged to the full ABS, which is reproduced by $l_{\text{inc}} = 2$ for the presently considered triple- ζ 3ZaPa-NR basis.

4.2 Performance in Larger Basis Sets

From the analysis of section 4.1 we observe that contraction thresholds $\epsilon \lesssim 10^{-4}$ afford suitably accurate total and atomization energies, while pruning HAM functions with eq. (2.6) also works well. In this section, we examine the accuracy of the compound procedure, where the ABS is both contracted and pruned of HAM functions.

Starting with the total energies shown in fig. 4.3, we observe for all OBSs that the ABS

can be contracted and pruned with eq. (2.6) with $l_{\text{inc}} = 1$ with negligible errors: as long as the contraction threshold $\epsilon \lesssim 10^{-5}$, the errors in the HF and MP2 total energies are of the order of $1 \mu E_h$ per electron or smaller.

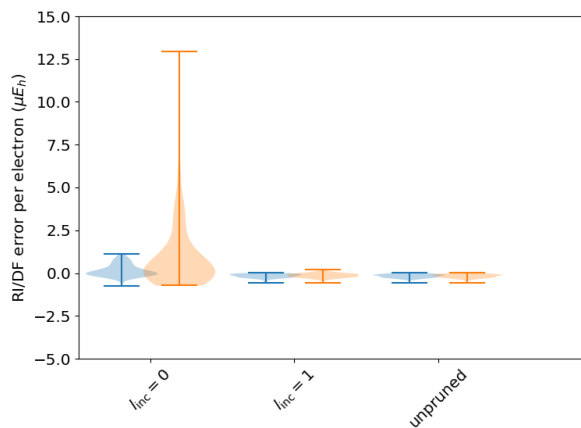
We also observe that for a fixed value of l_{inc} , the maximum RI/DF errors go down when the size of the OBS is increased. While $l_{\text{inc}} = 0$ leads to errors in the total energy of the order of $13 \mu E_h$ per electron with the triple- ζ 3ZaPa-NR OBS, the error decreases to $\mathcal{O}(4 \mu E_h)$ per electron in the quadruple- ζ 4ZaPa-NR OBS, and $\mathcal{O}(1 \mu E_h)$ per electron in the quintuple- ζ 5ZaPa-NR OBS.

Given that the increase in the size of the OBS is accompanied with an increase in the maximum angular momentum of the corresponding ABS (eq. (2.6)), a likely explanation for the decreasing error with increasing OBS is that the one-center approximation that is the cornerstone of the DF/RI method is becoming more accurate: energetically important two-center products of OBS functions are captured to better and better accuracy, when the ABS becomes richer in higher angular momentum functions.

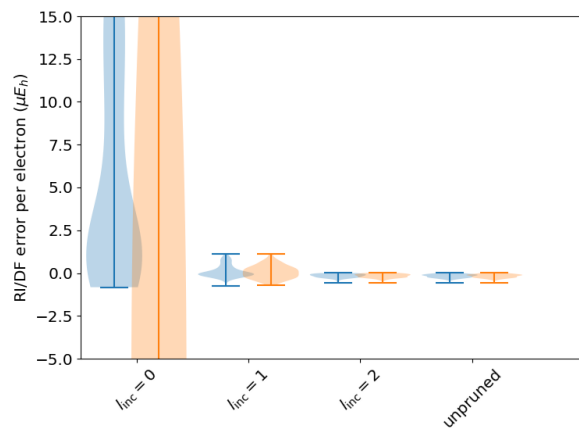
The corresponding results for atomization energies are shown in fig. 4.4. The errors in atomization energies of the order of cal/mol per atom are orders of magnitude smaller than the usual limit of chemical accuracy of 1 kcal/mol. We again note the increasing accuracy of the ABS with fixed l_{inc} in increasing size of the OBS, which is clear in the small- ϵ data for $l_{\text{inc}} = 0$. Excellent accuracy is achieved with $l_{\text{inc}} = 1$ and $\epsilon \lesssim 10^{-5}$ in all OBSs.

4.3 Size Reductions

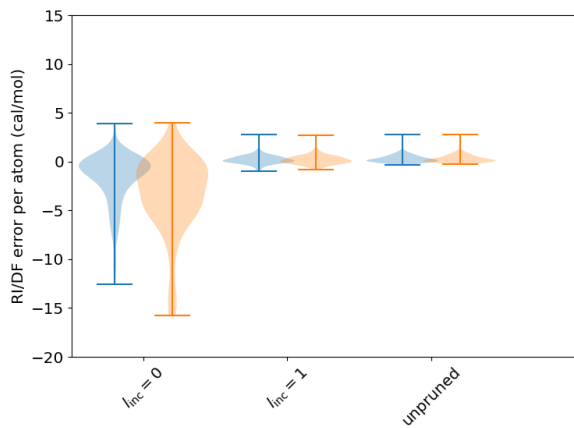
Having established that an excellent level of accuracy can be reached with the DF/RI approximation with the presently considered pruning and contraction technique for the automatically generated ABSs, we can proceed to discussing the associated reductions in the size of the ABS. As was already mentioned above, the computational cost of the DF/RI technique is linear in the size of the ABS; therefore, discussion on the cost of the DF/RI technique usually boils down



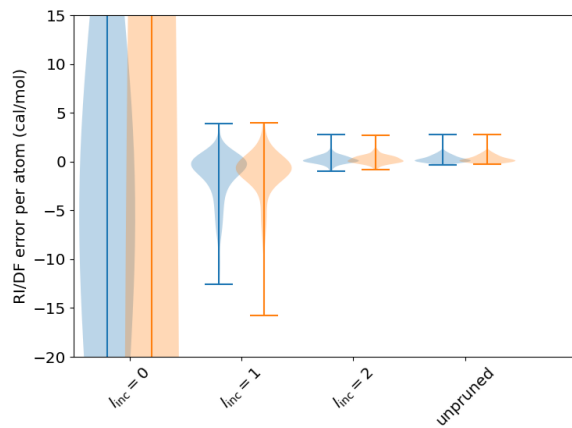
(a) Total energies, truncation with eq. (2.6)



(b) Total energies, truncation with eq. (2.7)

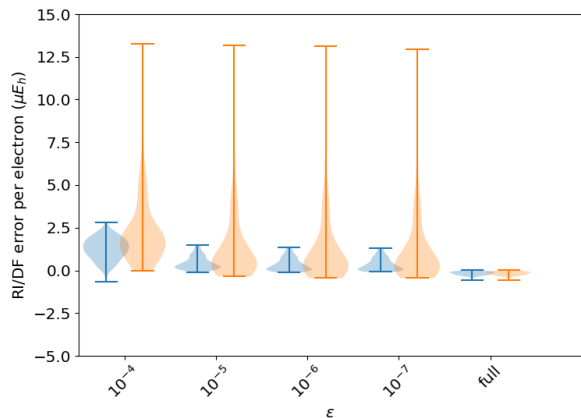


(c) Atomization energies, truncation with eq. (2.6)

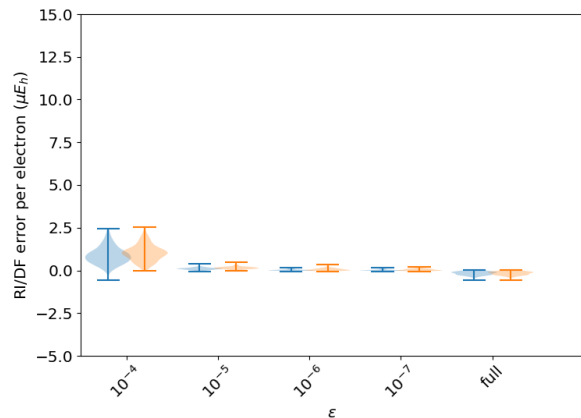


(d) Atomization energies, truncation with eq. (2.7)

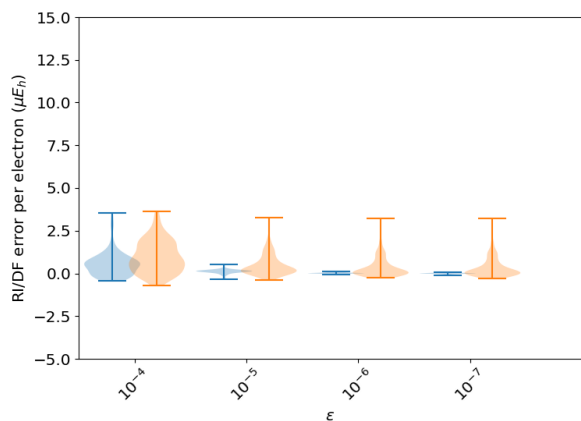
Figure 4.2: The effect of truncating high-angular-momentum functions according to eqs. (2.6) and (2.7) on the RI/DF errors HF and MP2 total and atomization energies of the studied molecules in the 3ZaPa-NR basis set. The last entries in the violin plots show the error distribution for the full, parent auxiliary basis set.



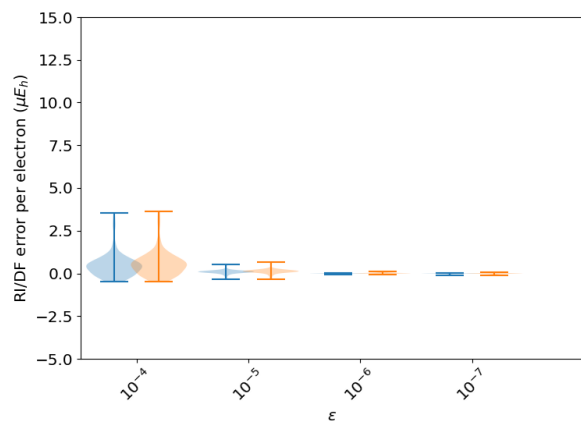
(a) 3ZaPa-NR, $l_{\text{inc}} = 0$



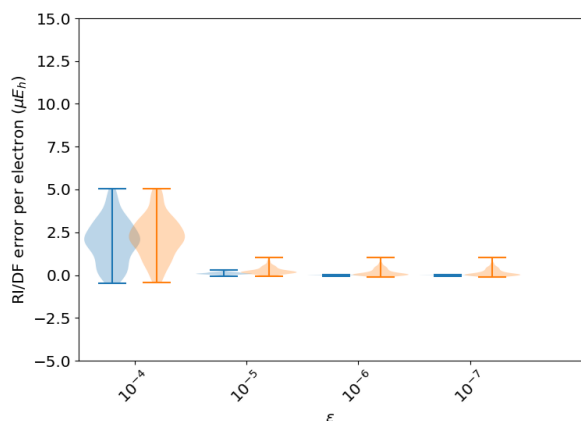
(b) 3ZaPa-NR, $l_{\text{inc}} = 1$



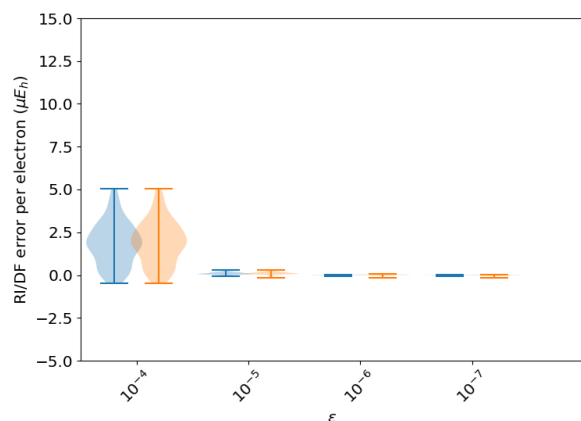
(c) 4ZaPa-NR, $l_{\text{inc}} = 0$



(d) 4ZaPa-NR, $l_{\text{inc}} = 1$

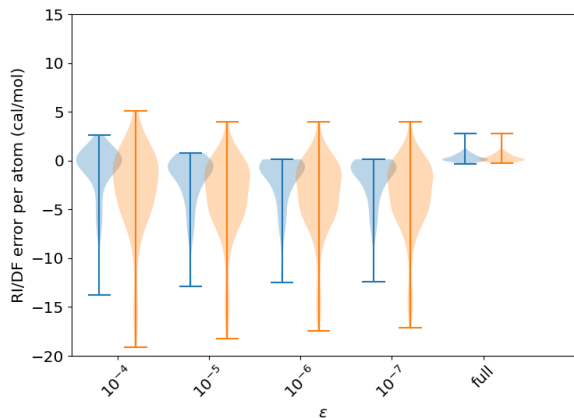


(e) 5ZaPa-NR, $l_{\text{inc}} = 0$

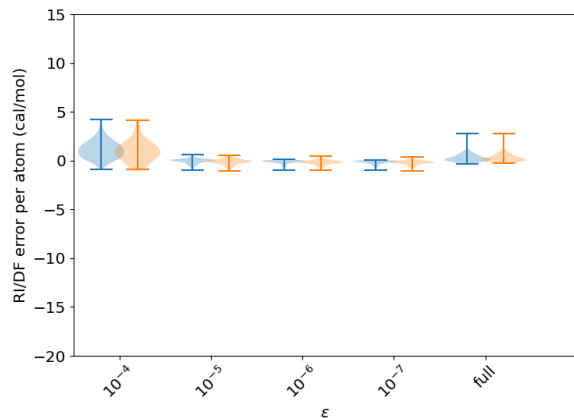


(f) 5ZaPa-NR, $l_{\text{inc}} = 1$

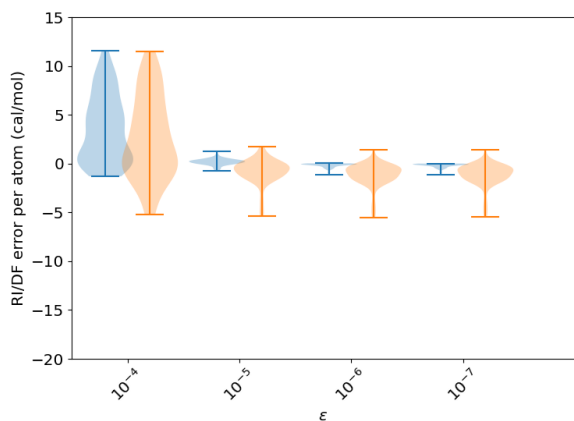
Figure 4.3: The effect of contraction on the RI/DF errors in the HF and MP2 total energies of the studied molecules in various basis sets, when the auxiliary basis is also truncated with eq. (2.6) with $l_{\text{inc}} = 0$ or $l_{\text{inc}} = 1$. The last entry in the 3ZaPa-NR plot shows the error distribution for the full, unpruned and uncontracted parent auxiliary basis set.



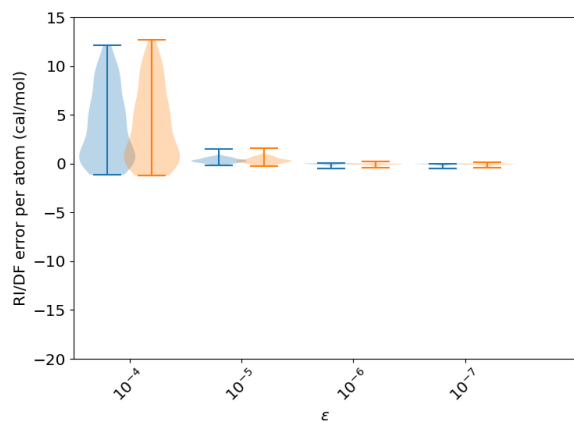
(a) 3ZaPa-NR, $l_{\text{inc}} = 0$



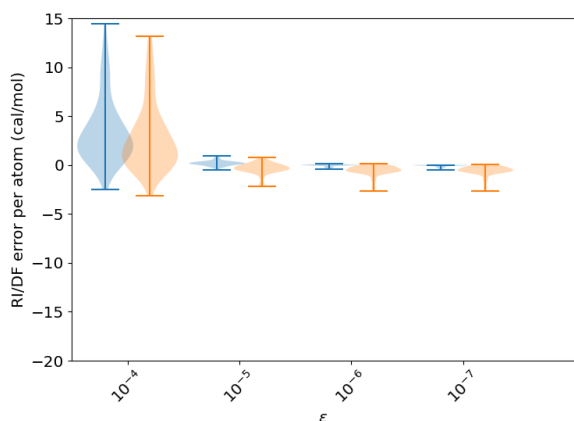
(b) 3ZaPa-NR, $l_{\text{inc}} = 1$



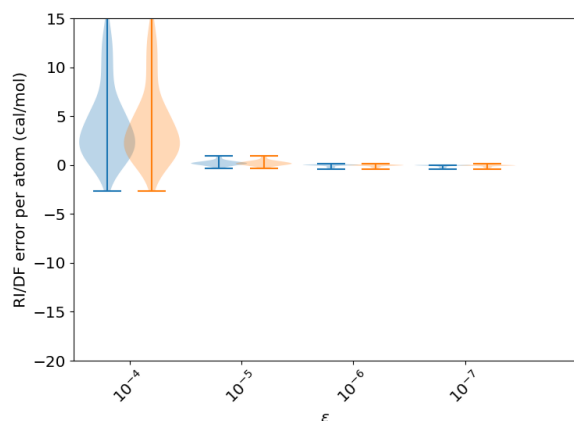
(c) 4ZaPa-NR, $l_{\text{inc}} = 0$



(d) 4ZaPa-NR, $l_{\text{inc}} = 1$



(e) 5ZaPa-NR, $l_{\text{inc}} = 0$



(f) 5ZaPa-NR, $l_{\text{inc}} = 1$

Figure 4.4: The effect of contraction on the RI/DF errors in the HF and MP2 atomization energies of the studied molecules in various basis sets, when the auxiliary basis is also truncated with eq. (2.6) with $l_{\text{inc}} = 0$ or $l_{\text{inc}} = 1$. The last entry in the 3ZaPa-NR plot shows the error distribution for the full, unpruned and uncontracted parent auxiliary basis set.

to the examination of the ratio

$$\gamma = N_{\text{ABS}}^{\text{bf}}/N_{\text{OBS}}^{\text{bf}}, \quad (4.1)$$

that is, the number of auxiliary functions divided by the number of orbital functions.

In the following, we will examine the accuracy and cost of automatically generated ABSs with the present method, considering truncation with $\epsilon \in [10^{-4}, 10^{-5}, 10^{-6}]$ and $l_{\text{inc}} \in [0, 1]$, which yielded good results above in section 4.2. We will compare the results to those of the AutoAux procedure of Stoychev et al.¹⁴.

The accuracy of these ABSs is shown in fig. 4.5. From these data, we can identify reasonable combinations of the truncation parameters, which appear to be balanced in the contraction and pruning of HAM functions. The choice $\epsilon = 10^{-4}$ and $l_{\text{inc}} = 0$ yields a “small” ABS, while $\epsilon = 10^{-5}$ and $l_{\text{inc}} = 1$ leads to a “large” ABS, and $\epsilon = 10^{-6}$ and $l_{\text{inc}} = 1$ yields a “verylarge” ABS.

The AutoAux basis is much more accurate for HF than for MP2 in large basis sets, and the method does not offer a straightforward way to improve the accuracy of the ABS. In contrast, these “small”, “large” and “verylarge” ABSs provide a sequence of improving accuracy in all studied OBSs, and with the exclusion of the “small” ABS in the 3ZaPa-NR OBS, they afford similar accuracy at both HF and MP2 levels of theory.

The ratios γ defined by eq. (4.1) for the various ABSs are shown in fig. 4.6, where the size of the full, untruncated autogenerated ABS is also shown for reference. The minimum and maximum values of γ are also given in table 1 for all OBSs and ABSs.

As was already discussed in ref. 15, the full autogenerated auxiliary basis sets are large: we see from fig. 4.6 and table 1 that the ratio γ varies from 8 to 12 in the full ABS. However, we also see that the contraction and pruning procedure of this work leads to significant reductions in the size of the ABSs.

Already going from the full ABS to the “verylarge” ABS is seen to roughly halve the number of auxiliary functions, indicating potential for significant savings with negligible errors as

shown by the related accuracy data in fig. 4.5.

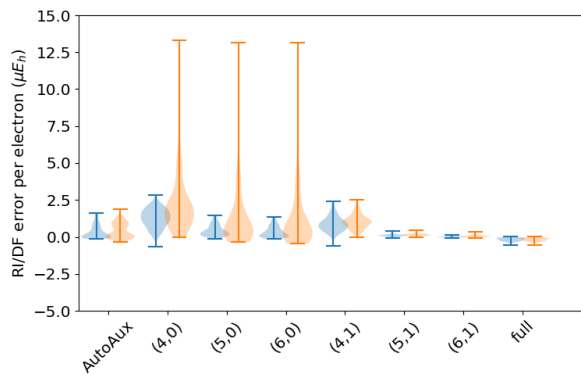
A further reduction is achieved by going to the “large” ABS, which still affords consistently small errors (fig. 4.5). The “small” ABS, in turn, exhibits γ in the range 3–4 for all OBSs, enabling quick calculations with somewhat larger errors, which may still be sufficiently small for practical applications.

5 Summary and Discussion

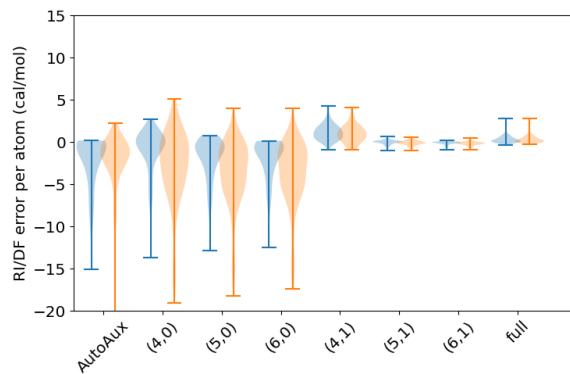
We have described an automated scheme for contracting auxiliary basis sets (ABSs) for a given orbital basis set. The scheme works with any type of atomic basis functions: in addition to the Gaussian-type orbitals (GTOs) considered in this work, the scheme can straightforwardly be applied also to other types of atomic basis functions, as the required atomic integrals can be readily be computed by quadrature.

In this work, we used the scheme of ref. 15 to generate the full auxiliary basis, which was then contracted and pruned of high-angular momentum (HAM) functions to produce computationally efficient ABSs. The scheme of ref. 15 employs a pivoted Cholesky decomposition of the electron repulsion integral (ERI) tensor to choose the subset of orbital products from which the auxiliary basis functions are chosen with another pivoted Cholesky decomposition. When applied with a Gaussian-type orbital (GTO) basis set, the prescreening of the orbital products with the pivoted Cholesky of the ERIs decreases the number of primitive GTOs in the resulting auxiliary basis set, leading to better computational efficiency even when the ABS is contracted.

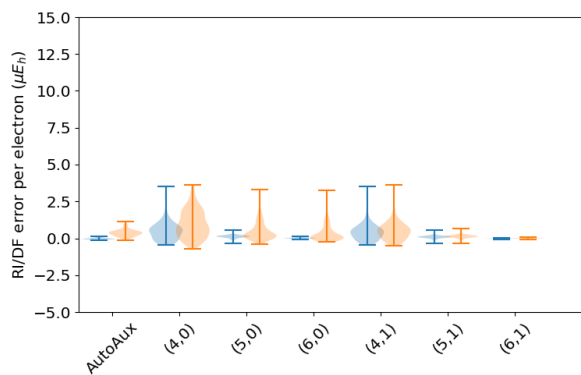
However, we find that the truncated auxiliary basis set obtained with the singular value decomposition (SVD) of eq. (2.4) comes out similar even if the initial pivoted Cholesky decomposition of the ERIs is not performed; that is, when the full set of orbital products is employed to generate the auxiliary functions. The present scheme thus appears to reproduce a similar number of contracted auxiliary functions regardless of whether any initial screening of orbital products is done.



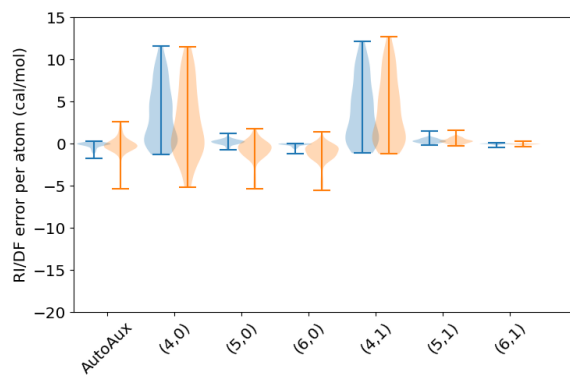
(a) 3ZaPa-NR total energies



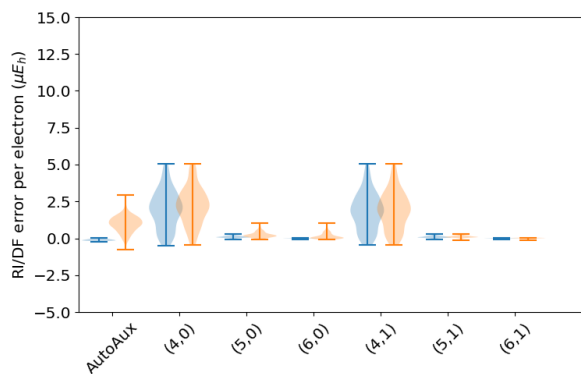
(b) 3ZaPa-NR atomization energies



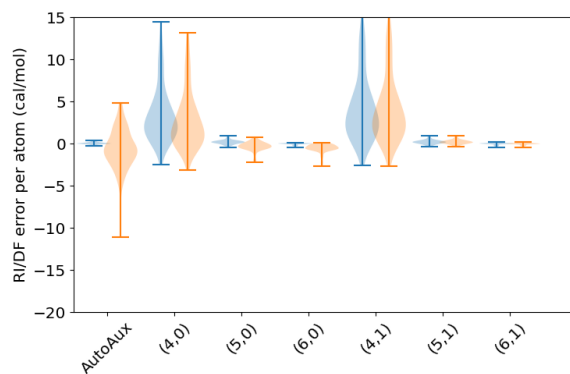
(c) 4ZaPa-NR total energies



(d) 4ZaPa-NR atomization energies

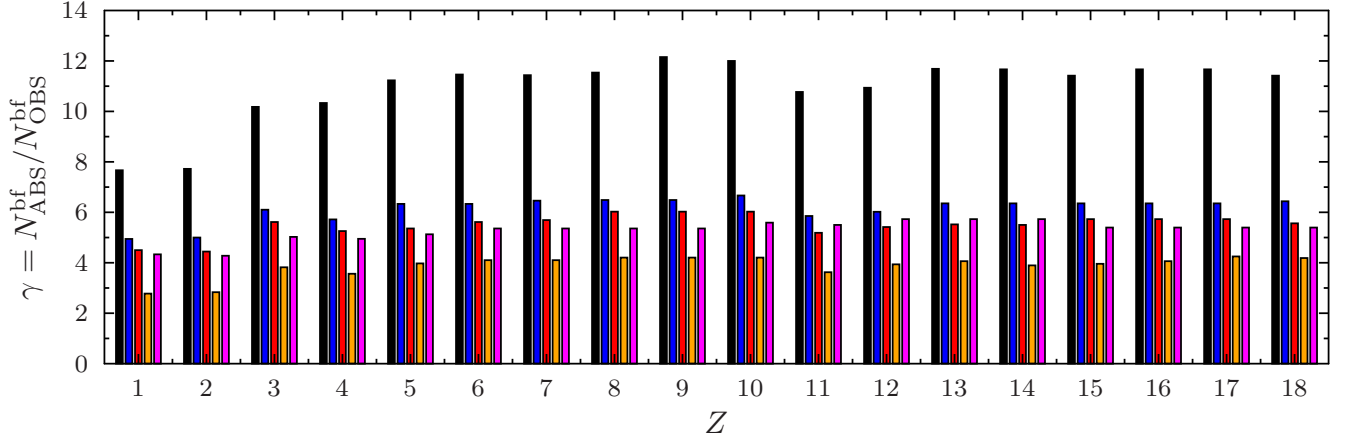


(e) 5ZaPa-NR total energies

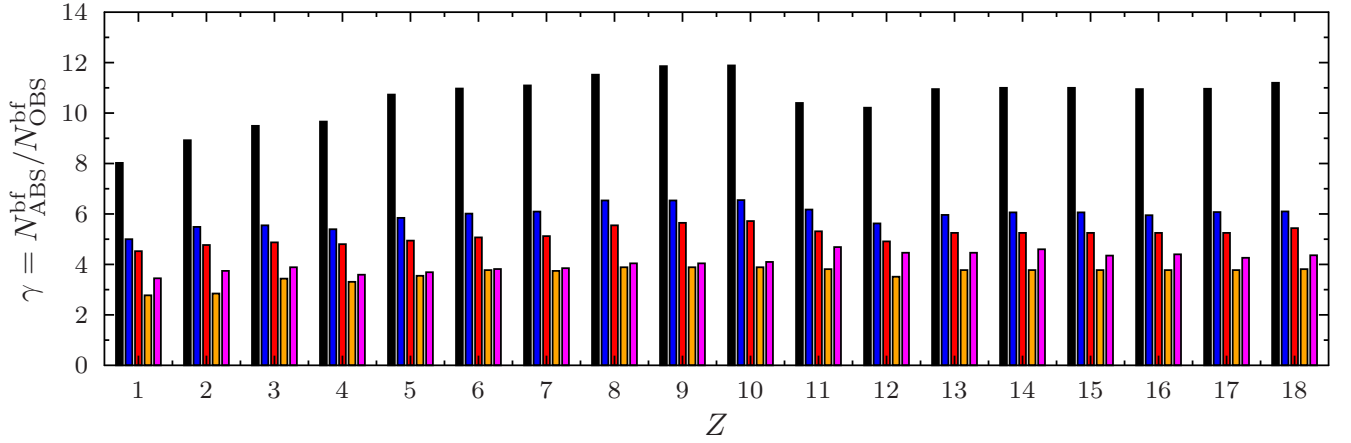


(f) 5ZaPa-NR atomization energies

Figure 4.5: Summary of the performance of the various automated schemes for automated auxiliary basis set construction across various orbital basis sets: the AutoAux procedure of Stoychev et al.¹⁴, as well as contracted and truncated basis sets with the parameters ϵ^{-x} and $l_{\text{inc}} = y$ specified with the shorthand (x, y) . The last entry in the 3ZaPa-NR plot shows the error distribution for the full, unpruned and uncontracted parent auxiliary basis set.



(a) 3ZaPa-NR



(b) 4ZaPa-NR

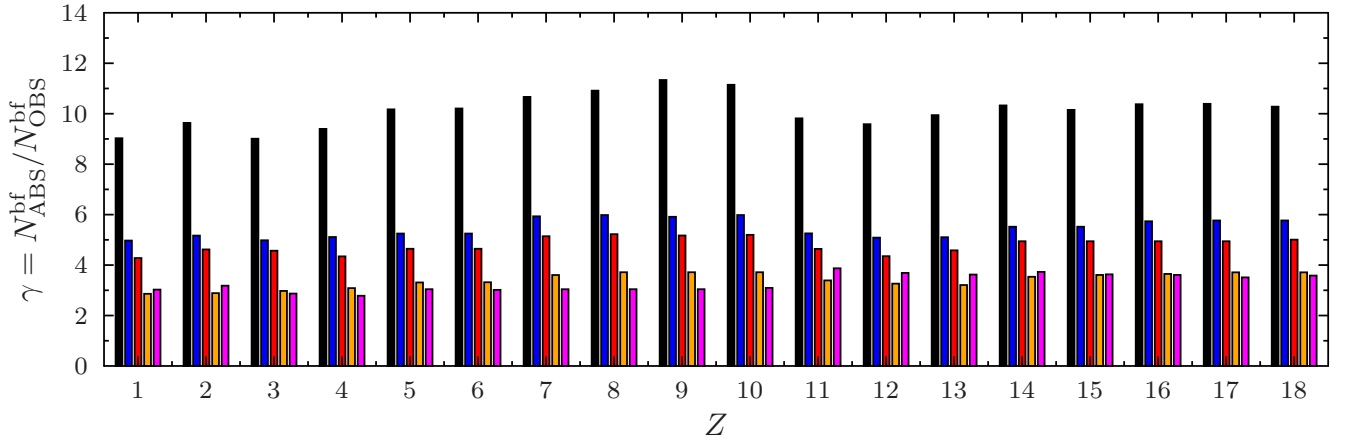


Figure 4.6: Sizes of autogenerated auxiliary basis for 3ZaPa-NR, 4ZaPa-NR, and 5ZaPa-NR for H–Ar. Reading in order from the left, the original primitive auxiliary basis set, generated by the procedure of ref. 15 is shown in black. The verylarge ($\epsilon = 10^{-6}$ and $l_{\text{inc}} = 1$), large ($\epsilon = 10^{-5}$ and $l_{\text{max}} = 1$), and small ($\epsilon = 10^{-4}$ and $l_{\text{max}} = 0$) auxiliary sets are shown in blue, red, and orange, respectively. For comparison, the size of the ABS generated with the AutoAux procedure of Stoychev et al.¹⁴ is shown in magenta.

Table 1: Ranges of γ defined by eq. (4.1) of various automatically generated ABSs.

	full		"verylarge"		"large"		"small"		AutoAux	
	min γ	max γ								
3ZaPa-NR	7.7	12.2	4.9	6.7	4.4	6.0	2.8	4.2	4.3	5.7
4ZaPa-NR	8.0	11.9	5.0	6.5	4.5	5.7	2.8	3.9	3.5	4.7
5ZaPa-NR	9.0	11.3	5.0	6.0	4.3	5.2	2.9	3.7	2.8	3.9

Although GTOs incur additional cost from contractions, as their integrals are usually evaluated in terms of Gaussian primitives, if numerical atomic orbitals (NAOs) are used, the present scheme becomes especially interesting. As NAO integrals are evaluated by quadrature, the linear transformation of the input auxiliary functions can be simply carried out to their expansion coefficients; the initialization with the pivoted Cholesky of the ERIs to choose the product functions is therefore not needed in the context of NAO calculations. We therefore believe that in addition to the application of the present method to Gaussian-type orbital (GTO) basis sets presented in this work, our scheme will be found to be extremely useful for NAO based calculations, as well.

Appendix: Conversion of Contraction Coefficients

From the eigendecomposition, one obtains eigenvectors in terms of Coulomb normalized primitives $\sum_A C_A^C N_A^C \phi_A(\mathbf{r})$, while basis set input is handled in typical programs in terms of overlap normalized primitives $\sum_A C_A^o N_A^o \phi_A(\mathbf{r})$. Denoting the two normalization coefficients as $N_A^C = (A|A)^{-1/2}$ and $N_A^o = \langle A|A \rangle^{-1/2}$, where the overlap of two unnormalized Gaussian primitives is³²

$$\langle A|B \rangle = \frac{1}{2} \Gamma \left(l + \frac{3}{2} \right) (\alpha_A + \alpha_B)^{-l-3/2} \delta_{u_A} \delta_{u_B} \quad (5.1)$$

and the Coulomb overlap is given by¹⁵

$$(A|B) = \frac{1}{4} \Gamma \left(l + \frac{3}{2} \right) \frac{(\alpha_A + \alpha_B)^{-l-1/2}}{\alpha_A \alpha_B} \delta_{u_A} \delta_{u_B}, \quad (5.2)$$

one finds the ratio

$$(A|B) = \frac{\alpha_A + \alpha_B}{2\alpha_A\alpha_B} \langle A|B \rangle \quad (5.3)$$

from which the coefficient follows as

$$C_A^o = \frac{N_A^o}{N_A^C} C_A^C = \sqrt{\frac{(A|A)}{\langle A|A \rangle}} C_A^C = \alpha_A^{1/2} C_A^C,$$

that is, the coefficients are multiplied by the square root of the corresponding exponent.

Acknowledgments

We thank the Academy of Finland for financial support under project numbers 350282 and 353749. We thank CSC – IT Centre for Science (Espoo, Finland) for computational resources.

References

- (1) Whitten, J. L. Coulombic potential energy integrals and approximations. *J. Chem. Phys.* **1973**, *58*, 4496.
- (2) Baerends, E. J.; Ellis, D. E.; Ros, P. Self-consistent molecular Hartree–Fock–Slater calculations I. The computational procedure. *Chem. Phys.* **1973**, *2*, 41–51.
- (3) Dunlap, B. I.; Connolly, J. W. D.; Sabin, J. R. On the applicability of LCAO- $X\alpha$ methods to molecules containing transition metal atoms: The nickel atom and nickel hydride. *Int. J. Quantum Chem.* **1977**, *12*, 81–87.
- (4) Dunlap, B. I.; Connolly, J. W. D.; Sabin, J. R. On some approximations in

- applications of $X\alpha$ theory. *J. Chem. Phys.* **1979**, *71*, 3396.
- (5) Dunlap, B. I.; Rösch, N.; Trickey, S. B. Variational fitting methods for electronic structure calculations. *Mol. Phys.* **2010**, *108*, 3167–3180.
 - (6) Vahtras, O.; Almlöf, J.; Feyereisen, M. W. Integral approximations for LCAO-SCF calculations. *Chem. Phys. Lett.* **1993**, *213*, 514–518.
 - (7) Smith, D. G. A.; Burns, L. A.; Simmonett, A. C.; Parrish, R. M.; Schieber, M. C.; Galvelis, R.; Kraus, P.; Kruse, H.; Di Remigio, R.; Alenaizan, A.; James, A. M.; Lehtola, S.; Misiewicz, J. P.; Scheurer, M.; Shaw, R. A.; Schriber, J. B.; Xie, Y.; Glick, Z. L.; Sirianni, D. A.; O’Brien, J. S.; Waldrop, J. M.; Kumar, A.; Hohenstein, E. G.; Pritchard, B. P.; Brooks, B. R.; Schaefer, H. F.; Sokolov, A. Y.; Patkowski, K.; DePrince, A. E.; Bozkaya, U.; King, R. A.; Evangelista, F. A.; Turney, J. M.; Crawford, T. D.; Sherrill, C. D. PSI4 1.4: Open-source software for high-throughput quantum chemistry. *J. Chem. Phys.* **2020**, *152*, 184108.
 - (8) Shiozaki, T. BAGEL: Brilliantly Advanced General Electronic-structure Library. *Wiley Interdiscip. Rev. Comput. Mol. Sci.* **2018**, *8*, e1331.
 - (9) Geudtner, G.; Calaminici, P.; Carmona-Espíndola, J.; del Campo, J. M.; Domínguez-Soria, V. D.; Moreno, R. F.; Gamboa, G. U.; Goursot, A.; Köster, A. M.; Reveles, J. U.; Mineva, T.; Vásquez-Pérez, J. M.; Vela, A.; Zúñiga-Gutierrez, B.; Salahub, D. R. deMon2k. *Wiley Interdiscip. Rev. Comput. Mol. Sci.* **2012**, *2*, 548–555.
 - (10) Aquilante, F.; Lindh, R.; Pedersen, T. B. Unbiased auxiliary basis sets for accurate two-electron integral approximations. *J. Chem. Phys.* **2007**, *127*, 114107.
 - (11) Yang, R.; Rendell, A. P.; Frisch, M. J. Automatically generated Coulomb fitting basis sets: design and accuracy for systems containing H to Kr. *J. Chem. Phys.* **2007**, *127*, 074102.
 - (12) Aquilante, F.; Gagliardi, L.; Pedersen, T. B.; Lindh, R. Atomic Cholesky decompositions: a route to unbiased auxiliary basis sets for density fitting approximation with tunable accuracy and efficiency. *J. Chem. Phys.* **2009**, *130*, 154107.
 - (13) Ren, X.; Rinke, P.; Blum, V.; Wieferink, J.; Tkatchenko, A.; Sanfilippo, A.; Reuter, K.; Scheffler, M. Resolution-of-identity approach to Hartree–Fock, hybrid density functionals, RPA, MP2 and GW with numeric atom-centered orbital basis functions. *New J. Phys.* **2012**, *14*, 053020.
 - (14) Stoychev, G. L.; Auer, A. A.; Neese, F. Automatic Generation of Auxiliary Basis Sets. *J. Chem. Theory Comput.* **2017**, *13*, 554–562.
 - (15) Lehtola, S. Straightforward and Accurate Automatic Auxiliary Basis Set Generation for Molecular Calculations with Atomic Orbital Basis Sets. *J. Chem. Theory Comput.* **2021**, *17*, 6886–6900.
 - (16) Pedersen, T. B.; Galván, I. F.; Lindh, R. The versatility of Cholesky decomposition of electron repulsion integrals. **2023**,
 - (17) Beebe, N. H. F.; Linderberg, J. Simplifications in the Two-Electron Integral Array in Molecular Calculations. *Int. J. Quant. Chem.* **1977**, *12*, 683–705.
 - (18) Lehtola, S. Curing basis set overcompleteness with pivoted Cholesky decompositions. *J. Chem. Phys.* **2019**, *151*, 241102.
 - (19) Lehtola, S. Accurate reproduction of strongly repulsive interatomic potentials. *Phys. Rev. A* **2020**, *101*, 032504.

- (20) Lehtola, S. A review on non-relativistic, fully numerical electronic structure calculations on atoms and diatomic molecules. *Int. J. Quantum Chem.* **2019**, *119*, e25968.
- (21) Lehtola, S. Fully numerical Hartree–Fock and density functional calculations. I. Atoms. *Int. J. Quantum Chem.* **2019**, *119*, e25945.
- (22) Kállay, M. A systematic way for the cost reduction of density fitting methods. *J. Chem. Phys.* **2014**, *141*, 244113.
- (23) Weigend, F. Hartree–Fock exchange fitting basis sets for H to Rn. *J. Comput. Chem.* **2008**, *29*, 167–175.
- (24) Manni, G. L.; Galván, I. F.; Alavi, A.; Aleotti, F.; Aquilante, F.; Autschbach, J.; Avagliano, D.; Baiardi, A.; Bao, J. J.; Battaglia, S.; Birnoschi, L.; Blanco-González, A.; Bokarev, S. I.; Broer, R.; Cacciari, R.; Calio, P. B.; Carlson, R. K.; Couto, R. C.; Cerdán, L.; Chibotaru, L. F.; Chilton, N. F.; Church, J. R.; Conti, I.; Coriani, S.; Cuéllar-Zuquin, J.; Daoud, R. E.; Dattani, N.; Decleva, P.; de Graaf, C.; Delcey, M. G.; Vico, L. D.; Dobrautz, W.; Dong, S. S.; Feng, R.; Ferré, N.; Filatov(Gulak), M.; Gagliardi, L.; Garavelli, M.; González, L.; Guan, Y.; Guo, M.; Hennefarth, M. R.; Hermes, M. R.; Hoyer, C. E.; Huix-Rotllant, M.; Jaiswal, V. K.; Kaiser, A.; Kaliakin, D. S.; Khamesian, M.; King, D. S.; Kochetov, V.; Krośnicki, M.; Kumaar, A. A.; Larsson, E. D.; Lehtola, S.; Lepetit, M.-B.; Lischka, H.; Ríos, P. L.; Lundberg, M.; Ma, D.; Mai, S.; Marquetand, P.; Merritt, I. C. D.; Montorsi, F.; Mörchen, M.; Nenov, A.; Nguyen, V. H. A.; Nishimoto, Y.; Oakley, M. S.; Olivucci, M.; Oppel, M.; Padula, D.; Pandharkar, R.; Phung, Q. M.; Plasser, F.; Raggi, G.; Rebolini, E.; Reiher, M.; Rivalta, I.; Roca-Sanjuán, D.; Romig, T.; Safari, A. A.; Sánchez-Mansilla, A.; Sand, A. M.; Schapiro, I.; Scott, T. R.; Segarra-Martí, J.; Segatta, F.; Sergentu, D.-C.; Sharma, P.; Shepard, R.; Shu, Y.; Staab, J. K.; Straatsma, T. P.; Sørensen, L. K.; Tenorio, B. N. C.; Truhlar, D. G.; Ungur, L.; Vacher, M.; Veryazov, V.; Voß, T. A.; Weser, O.; Wu, D.; Yang, X.; Yarkony, D.; Zhou, C.; Zobel, J. P.; Lindh, R. The OpenMolcas Web: A Community-Driven Approach to Advancing Computational Chemistry. *J. Chem. Theory Comput.* **2023**,
- (25) Ranasinghe, D. S.; Petersson, G. A. CCSD(T)/CBS atomic and molecular benchmarks for H through Ar. *J. Chem. Phys.* **2013**, *138*, 144104.
- (26) Pritchard, B. P.; Altarawy, D.; Didier, B.; Gibson, T. D.; Windus, T. L. New Basis Set Exchange: An Open, Up-to-Date Resource for the Molecular Sciences Community. *J. Chem. Inf. Model.* **2019**, *59*, 4814–4820.
- (27) Lehtola, J.; Hakala, M.; Sakko, A.; Hämäläinen, K. ERKALE – A flexible program package for X-ray properties of atoms and molecules. *J. Comput. Chem.* **2012**, *33*, 1572–1585.
- (28) Lehtola, S. ERKALE – HF/DFT from Hel. 2023; <https://github.com/susilehtola/erkale>, Accessed 23 March 2023.
- (29) Karton, A.; Sylvetsky, N.; Martin, J. M. L. W4-17: A diverse and high-confidence dataset of atomization energies for benchmarking high-level electronic structure methods. *J. Comput. Chem.* **2017**, *38*, 2063–2075.
- (30) Weigend, F.; Ahlrichs, R. Balanced basis sets of split valence, triple zeta valence and quadruple zeta valence quality for H to Rn: Design and assessment of accuracy. *Phys. Chem. Chem. Phys.* **2005**, *7*, 3297–305.
- (31) Frisch, M. J.; Trucks, G. W.; Schlegel, H. B.; Scuseria, G. E.;

Robb, M. A.; Cheeseman, J. R.; Scalmani, G.; Barone, V.; Petersson, G. A.; Nakatsuji, H.; Li, X.; Caricato, M.; Marenich, A. V.; Bloino, J.; Janesko, B. G.; Gomperts, R.; Mennucci, B.; Hratchian, H. P.; Ortiz, J. V.; Izmaylov, A. F.; Sonnenberg, J. L.; Williams-Young, D.; Ding, F.; Lipparini, F.; Egidi, F.; Goings, J.; Peng, B.; Petrone, A.; Henderson, T.; Ranasinghe, D.; Zakrzewski, V. G.; Gao, J.; Rega, N.; Zheng, G.; Liang, W.; Hada, M.; Ehara, M.; Toyota, K.; Fukuda, R.; Hasegawa, J.; Ishida, M.; Nakajima, T.; Honda, Y.; Kitao, O.; Nakai, H.; Vreven, T.; Throssell, K.; Montgomery Jr., J. A.; Peralta, J. E.; Ogliaro, F.; Bearpark, M. J.; Heyd, J. J.; Brothers, E. N.; Kudin, K. N.; Staroverov, V. N.; Keith, T. A.; Kobayashi, R.; Normand, J.; Raghavachari, K.; Rendell, A. P.; Burant, J. C.; Iyengar, S. S.; Tomasi, J.; Cossi, M.; Millam, J. M.; Klene, M.; Adamo, C.; Cammi, R.; Ochterski, J. W.; Martin, R. L.; Morokuma, K.; Farkas, O.; Foresman, J. B.; Fox, D. J. Gaussian 16 Revision B.01. 2016.

- (32) Lehtola, S. Polarized Gaussian basis sets from one-electron ions. *J. Chem. Phys.* **2020**, *152*, 134108.

TOC Graphic

